Structure, Vol. 11, 875–885, July, 2003, ©2003 Elsevier Science Ltd. All rights reserved. DOI 10.1016/S0969-2126(03)00131-X

The Crystal Structure of Human Angiogenin in Complex with an Antitumor Neutralizing Antibody

Gayatri B. Chavali,[1,5,6]
Anastassios C. Papageorgiou,[1,5,7]
Karen A. Olson,[2] James W. Fett,[2] Guo-fu Hu,[2,4]
Robert Shapiro,[2,3] and K. Ravi Acharya[1,*]
[1]Department of Biology and Biochemistry
University of Bath
Claverton Down
Bath BA2 7AY
United Kingdom
[2]Center for Biochemical and Biophysical Sciences and Medicine
[3]Department of Pathology
[4]Department of Radiology
Harvard Medical School
One Kendall Square
Cambridge, Massachusetts 02139

Summary

The murine monoclonal antibody 26-2F neutralizes the angiogenic and ribonucleolytic activities of human angiogenin (ANG) and is highly effective in preventing the establishment and metastatic dissemination of human tumors in athymic mice. Here we report a 2.0 Å resolution crystal structure for the complex of ANG with the Fab fragment of 26-2F that reveals the detailed interactions between ANG and the complementarity-determining regions (CDRs) of the antibody. Surprisingly, Fab binding induces a dramatic conformational change in the cell binding region of ANG at the opposite end of the molecule from the combining site; cross-linking experiments indicate that this rearrangement also occurs in solution. The ANG-Fab complex structure should be invaluable for designing maximally humanized versions of 26-2F for potential clinical use.

Introduction

Angiogenin (ANG) is a secreted, single-chain 14,143 Da protein that induces angiogenesis in vivo (Riordan, 1997; Adams and Subramanian, 1999). It was isolated originally from medium conditioned by human colon carcinoma cells (Fett et al., 1985) and subsequently from normal serum and milk (Shapiro et al., 1987; Maes et al., 1988). ANG is a member of the pancreatic RNase superfamily and possesses a ribonucleolytic activity (Shapiro et al., 1986) that is necessary for its blood vessel-inducing capability (Shapiro et al., 1989; Shapiro and Vallee 1989). The three-dimensional structures of human (Acharya et al., 1994; Lequin et al., 1997; Leonidas et al., 1999) and bovine ANG (Acharya et al., 1995; Lequin et al., 1996) have been determined. Although the fold of the protein is similar to those of pancreatic RNase A and other homologs, ANG contains unique structural features that account for its characteristic enzymatic and angiogenic activities.

ANG is produced by many distinct types of human tumor cells grown in culture (Fett et al., 1985; Rybak et al., 1987; Adams and Subramanian, 1999), and, in several studies, its expression has been positively correlated with cancer progression and poor prognosis (e.g., Li et al., 1994; Shimoyama et al., 1996; Eberle et al., 2000). It has therefore been of interest to identify inhibitors of the functions of ANG and to evaluate their potential utility in the treatment and/or prevention of cancer. One of the earliest antagonists was the murine monoclonal antibody (mAb) 26-2F. It is an IgG1κ, with an IC_{50} binding affinity of 1.6 nM, that neutralizes the ribonucleolytic, angiogenic, and mitogenic activities of human ANG (Fett et al., 1994; Hu et al., 1997).

Preclinical studies have shown that mAb 26-2F is remarkably effective in preventing the establishment of primary (Olson et al., 1994, 1995) and metastatic human tumors (Olson et al., 2002) of various histological types in athymic mice. Thus, immunotherapeutic neutralization of ANG might be a powerful broad-spectrum anticancer approach. However, repeated use of murine antibodies for the treatment of human disease can elicit undesirable antimouse immune responses (Levy and Miller, 1983; Lobuglio et al., 1986). In order to minimize these side effects, we initially constructed a chimeric version of mAb 26-2F, in which the murine constant (C) region segments have been replaced through genetic engineering with human immunoglobulin sequences (Piccoli et al., 1998). In a mouse model for breast cancer establishment, the antitumor activity of this antibody is identical to that of its murine counterpart. Although chimeric antibodies have reduced immunogenicity, patients treated with them have developed untoward immune responses that are directed against the remaining mouse variable (V) region residues (Choy et al., 1993, 1994). As a result, humanized versions of murine mAbs are emerging as preferred therapeutics. In contrast to chimerized IgG antibodies, which still contain ~33% mouse sequences, humanized IgG counterparts may contain less than 5% of unwanted murine residues. Several of these derivatives have now entered clinical trials (Carter, 2001).

A typical strategy used to construct humanized antibodies is to graft murine complementarity-determining regions (CDRs) into consensus human framework regions (Presta et al., 1997). However, this process often results in antibody products exhibiting less than optimal binding characteristics (Queen et al., 1989; Foote and Winter, 1992). A procedure of trial and error is then required, in which CDR regions are manipulated and selected murine-derived framework residues are incorporated to maintain or enhance the binding affinity of the parent antibody (Riechmann et al., 1988). As an alternative, we have opted to pursue our goal of engineering

*Correspondence: k.r.acharya@bath.ac.uk
[5]These authors contributed equally to this work.
[6]Present address: Cambridge Institute of Medical Research, MRC/Wellcome Trust Building, Cambridge CB2 2XY, United Kingdom.
[7]Present Address: Turku Centre for Biotechnology, University of Turku and Åbo Akademi University, BioCity, Turku 20521, Finland.

Table 1. Crystallographic Statistics

Data Collection Statistics			
Space group	C2		
Cell parameters			
a × b × c (Å)	120.6 × 72.5 × 87		
β (°)	112.5		
Resolution range	40–2.0 Å		
Number of unique reflections	46,470		
Average I/σ(I)	17.6 (4.92)[a]		
Overall completeness (%)	98.9 (97.8)[a]		
R_{merge} (%)[b]	6.1 (20.0)[a]		
Diffraction Agreement			
Resolution	40.0–2.0 Å		
Model			
R_{cryst} (%)[c]	23.2		
R_{free} (%)[d]	27.2		
Total number of residues	562		
Contents of asymmetric unit	1 Fab-ANG complex		
Total number of protein atoms	4280		
Total number of water molecules	328		
Ions/ligands	8 sulfates and 6 glycerols		
Average B factor (Å^2)	39.7		
Average B Factors (Å^2) for Residues			
	Light Chain	Heavy Chain	ANG
Overall	37.6	41.4	37.1
Main chain	36.8	41.5	35.9
Side chain	38.5	41.3	38.2
Water molecules (average)	42.7		
Stereochemistry (Rmsd from Ideality)			
Bond lengths (Å)	0.009		
Bond angles (°)	1.8		
Dihedrals (°)	26.8		
Improper angles (°)	1.3		

[a] Outermost shell = 2.07–2.00 Å.
[b] $R_{merge} = \Sigma_h\Sigma_i|I(h) - I_i(h)|/\Sigma_h\Sigma_i I_i(h)$, where $I(h)$ and $I_i(h)$ are the mean and ith measurements of the intensity of reflection h, respectively.
[c] $R_{cryst} = \Sigma_h|F_o - F_c|/\Sigma_h F_o$, where F_o and F_c are the observed and calculated structure factor amplitudes of reflection h, respectively.
[d] R_{free} is equal to R_{cryst} for a randomly selected 5 % subset of reflections not used in the refinement.

humanized versions of mAb 26-2F by first determining the three-dimensional structure of the complex of the 26-2F Fab fragment with ANG. This structure reveals the details of the binding epitope and identifies framework residues that support the conformational integrity of the CDRs. Moreover, it indicates that neutralization of ANG function by the antibody is achieved through an unusual mechanism involving both direct interactions with the active site region and the induction of an extensive reorganization of the cell binding site at the opposite end of the ANG molecule. These findings should greatly facilitate the design of high-affinity humanized mAb 26-2F counterparts for use in the treatment of human cancers and other ANG-dependent diseases.

Results and Discussion

The structure of the ANG-Fab complex was determined at 2.0 Å resolution and refined to a crystallographic R factor of 23.2% (R_{free} = 27.2%). Details of the data processing and refinement statistics are given in Table 1. The crystallographic asymmetric unit contains a single 1:1 complex and is shown in Figure 1. Residues 128–133 in the C region of the Fab heavy (H) chain (Figure 2) could not be positioned unambiguously and were modeled as glycines. These residues are reported to be highly mobile in other antibody structures (Schneider et al., 1988; Sheriff et al., 1996). No density was observed for the side chain atoms of light (L) chain C region residues 198–199 and 210–211, H chain C region residues 134 and 213–215, and the N-terminal pyroglutamic acid (<Glu) of ANG; these were modeled as alanines. The refined model includes 562 protein residues, 328 water molecules, 8 sulfate ions, and 6 glycerol molecules. Analysis with PROCHECK (Laskowski et al., 1993) indicated that the ϕ-ψ conformational angles were within the limits expected for a structure at this resolution, with only one residue (L198) in the disallowed region of the Ramachandran plot (87.4% in the core). The electron density map indicated that there were three variations in the C regions with respect to the published consensus amino acid sequence for this antibody subclass (Kabat et al., 1991); residues 146 and 165 in the C_L region were identified as Arg and Gln, instead of Lys and Glu, respectively,

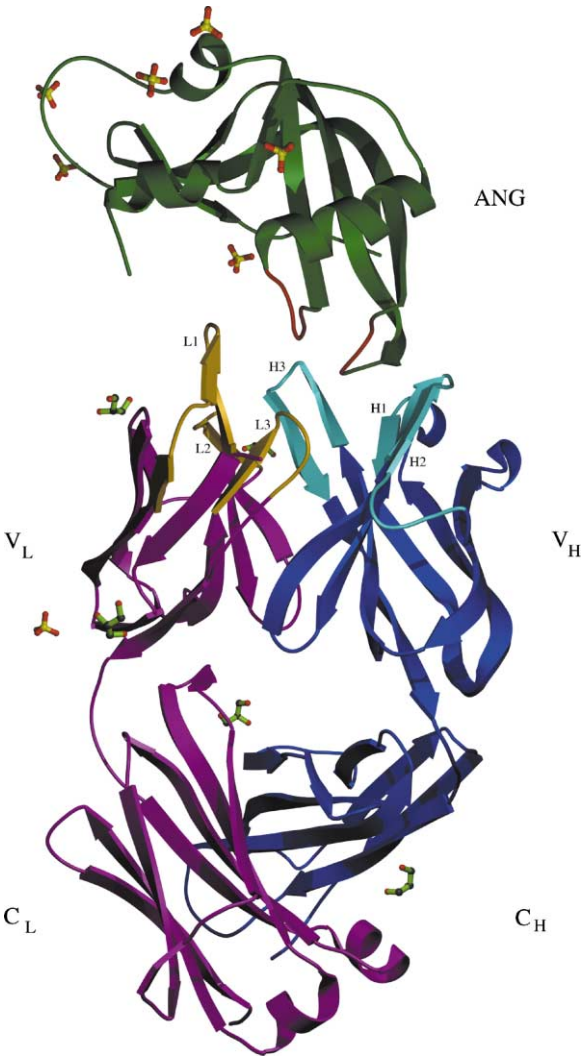

Figure 1. Structure of the Complex Formed between Human ANG and Fab 26-2F

The L and H chains of the Fab molecule are in magenta and blue, respectively, except for their CDRs (L1–L3 and H1–H3), which are in gold and cyan, respectively. ANG, green. Sulfate ions (yellow bonds) and glycerol molecules (green bonds) are also shown. The figure was generated with MOLSCRIPT (Kraulis, 1991).

and residue 189 in the C_H region was found to be Trp, instead of Arg. These residues are not located at the contact interface. Nine *cis*-prolines were identified in the structure, seven of which are in the Fab. Most of these appear to be conserved in the majority of mouse IgG1 sequences (Sheriff et al., 1996).

Overall Structure of the Complex

The conformation of Fab 26-2F closely resembles that of the Fab for murine monoclonal antibody D44.1 (also an IgG1κ) raised against hen egg white lysozyme (Protein Data Bank code 1MLB) (Braden et al., 1994). The two structures can be superposed with an rmsd of 1.64 Å (421 C^α atoms) (Figure 3). This value decreases only to 1.56 Å when the CDR regions are omitted. The separate V and C domains correspond more closely, with rmsd's of 1.27 Å and 0.79 Å, respectively. The elbow angles are 132.3° for 26-2F and 173.8° for D44.1; both are within the broad range of 125°–225° normally observed for Fab fragments (Wilson and Stanfield, 1994).

The six CDR loops of Fab 26-2F (L1, L2, and L3 from V_L and H1, H2, and H3 from V_H) are well defined in the electron density map. Although CDR sequences vary considerably from one antibody to another, most CDRs adopt one of a set of canonical structures. In Fab 26-2F, CDRs L1, L2, L3, H1, and H2 can be assigned to canonical classes 5, 1, 1, 1, and 3, respectively, described by Chothia and coworkers (Chothia and Lesk, 1987; Chothia et al., 1989; Al-Lazikani et al., 1997). CDR-H3 in antibodies is far more variable than the others in length, sequence, and conformation, and no canonical structures have been described for it, although certain regularities have been observed. Mas et al. (1992) have noted two types of backbone conformations at the base of the loop, kinked and extended, reflecting the presence and absence, respectively, of a bulge around the second residue from the C-terminal end. The 12-residue H3 loop of Fab 26-2F (H95–H102) has the more common kinked structure and forms both of the interactions usually associated with this conformation, i.e., a salt bridge between an Asp (H101) two residues from the C-terminal end and a framework Arg (H94) that immediately precedes the loop and a hydrogen bond between the carbonyl oxygen of the same Asp and the Nε1 atom of the highly conserved framework Trp (H103) that immediately follows the loop (Shirai et al., 1996; Morea et al., 1998). Three of the four tyrosines in CDR-H3 are involved in hydrophobic packing or stacking interactions with the light chain. H98 (Tyr) and H100b (Tyr) contact L32 (Phe) of CDR-L1, and H98 also interacts with L30b (Tyr) and L30d (Ile) of CDR-L1. H100 (Tyr) stacks against L49 (Tyr), the first framework residue on the N-terminal side of L2. Interactions with framework residues also appear to stabilize the conformation of CDR-H2; the side chain OH of H50 (Thr) hydrogen bonds with the Nε1 atom of H47 (Trp), and the main chain O of H52 (Ser) hydrogen bonds with Nη1 of H71 (Arg).

The structure of <Glu-1 ANG in the complex is similar to that of free ANG (Protein Data Bank code 1B1I; Leonidas et al., 1999), except for the cell binding region (detailed below). Superposition of 108 C^α atoms in the free and complexed proteins (i.e., excluding the three N-terminal and two C-terminal residues, as well as amino acids 59–68 in the cell binding site) resulted in an rmsd of 0.86 Å.

The Antigen-Antibody Interface

Fab 26-2F recognizes two discontinuous segments of ANG comprising residues 34–41 (segment I) and 85–91 (segment II); these segments lie on two surface loops that are juxtaposed in the three-dimensional structure (Figures 1 and 4) and are linked by the Cys39-Cys92 disulfide bridge. Five of the six CDRs of the Fab (i.e., all but L2) make contacts with ANG. Formation of the complex buries 1326 $Å^2$ of the solvent-accessible surface area of the proteins: 649 $Å^2$ for the antibody (38% from the L chain and 62% from the H chain) and 677 $Å^2$ for ANG (43% from segment I and 57% from segment

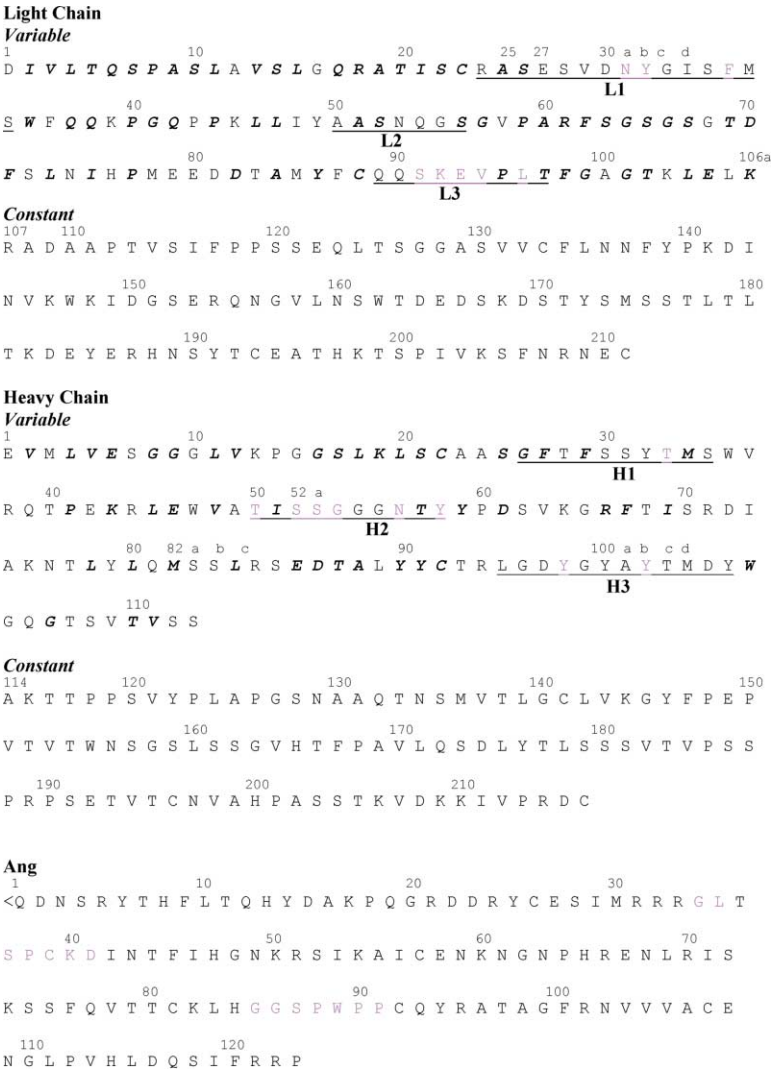

Figure 2. Amino Acid Sequences of Fab 26-2F and Human ANG

The antibody V region sequences are those deduced from the DNA sequence (Piccoli et al., 1998); GenBank accession numbers are AF039414 (V_L) and AF039415 (V_H). Residue numbering is that of Chothia and Lesk (1987). Residues that are highly conserved in this IgG subclass are shown in bold italic type. The six CDR loops as defined by the antibody modeling programs AbM (Oxford Molecular) and WAM (Whitelegg and Rees, 2000; https://antibody.bath.ac.uk/WAMpredict.html) are underlined; these definitions differ from those of Chothia and coworkers (Chothia and Lesk, 1987; Chothia et al. 1989; Al-Lazikani et al., 1997) only for CDRs H1 and H2. The DNA sequences for the C_L and C_H regions have not been determined; the amino acid sequences shown are those from MOPC 41 and MOPC 21, respectively (Kabat et al., 1991), except for three residues (L146, L165, and H89) where the crystal structure clearly reveals differences. The ANG sequence is from Strydom et al. (1985). Residues involved in intermolecular contacts are highlighted in magenta.

II). The total value is toward the lower end of the range reported for other complexes of Fab fragments with protein antigens (Davies and Cohen, 1996; Jones and Thornton, 1996). In all, 14 residues from ANG and 17 from the Fab participate in the interface, forming 81 van der Waals contacts (Table 2) and 13 potential hydrogen bonds (Table 3).

The shallow binding pocket on the surface of the antibody is formed by CDRs L1 and H3 on one side and L3, H2, and H1 on the other. Segments I and II of ANG fit snugly into this pocket (Figure 4); both segments have moved slightly from their positions in free ANG to optimize contacts with the Fab. The most extensively involved CDR is H2, which forms interactions with every

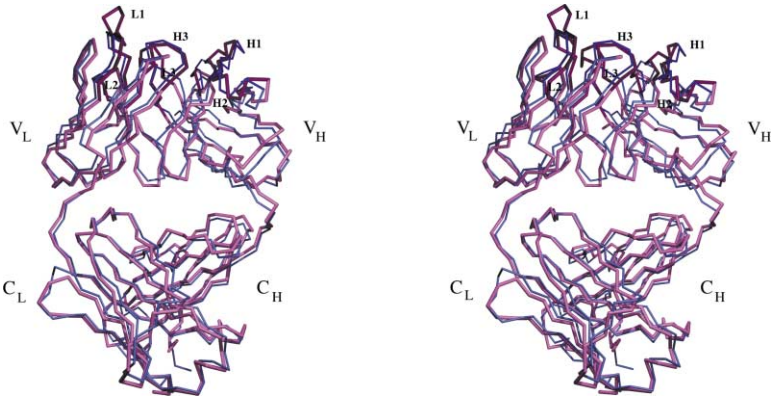

Figure 3. Stereo View of the Superposed C^α Backbones of the Fab Molecule from the ANG-Fab 26-2F Complex (Magenta) and Fab D44.1 (Protein Data Bank Code 1MLB; Blue)

The locations of the CDRs (L1–L3 and H1–H3) are indicated.

Table 2. Van der Waals Contacts between Fab and ANG in the Complex

Fab CDR	Fab Residue	ANG Residue	Number of Contacts
L1	Asn30a	Ser37	3
	Tyr30b	Gly34	1
		Leu35	7
		Ser37	1
		Pro38	4
		Lys40	3
	Phe32	Pro38	8
L3	Lys92	Ser37	2
		Pro38	1
	Glu93	Trp89	1
	Val94	Trp89	3
	Leu96	Trp89	5
H2	Thr50	Trp89	1
	Ser52	Gly85	1
		Gly86	1
	Ser52a	Gly85	1
		Gly86	1
	Gly53	Gly85	1
	Asn56	Ser87	1
		Pro91	2
	Tyr58	Ser87	1
		Pro88	2
		Trp89	9
		Pro90	1
H3	Tyr98	Cys39	1
		Lys40	2
		Asp41	8
	Tyr100b	Pro38	4
		Cys39	1
		Pro88	4

The program CONTACT (CCP4, 1994) was used for calculations (distance cutoffs: C-C, 4.1 Å; C-N, 3.8 Å; C-O, 3.7 Å; N-N, 3.4 Å; O-O, 3.3 Å; and O-N, 3.4 Å).

residue on segment II of ANG, including five hydrogen bonds with the main chain of this segment (Tables 2 and 3). CDR-L1 plays a similarly pivotal role vis-à-vis segment I of ANG, interacting with five of the seven contact residues and making three hydrogen bonds, again with main chain elements. (Indeed, it is striking that all but two of the hydrogen bonds of the Fab are with the main chain of ANG.) CDRs L3 and H3 contact both segments on ANG. The least utilized of the CDRs at the interface appears to be H1, which makes only a single interaction with ANG.

As observed in other antigen-antibody complexes (Padlan, 1990; Davies and Cohen, 1996; Sogabe et al., 1997), aromatic residues seem to play a major role in the binding of ANG to the Fab. The five aromatic interface residues on the Fab account for 66% of the total contacts, and Trp89 of ANG alone is involved in 23% of the interactions. Indeed, the most dominant feature of the interface is the complete burial of Trp89 in the antibody (the accessible surface area of this residue decreases from 181 $Å^2$ in free ANG to 0 $Å^2$ in the complex).

The interface contains 11 buried water molecules, none of which are involved in water-mediated hydrogen bonds between ANG and the Fab. However, two water molecules participate in a hydrogen-bonding network that extends from Gly86 O of ANG to H98 (Tyr) N and H102b (Tyr) OH of the Fab. The sulfate ions identified in the structure are not at the binding interface, although two interact with residues that also form intermolecular contacts (Lys40 of ANG and residue 52a [Ser] on CDR-H2).

Correlation of Structural Data with Results from Epitope-Mapping Studies on mAb 26-2F

mAb 26-2F was shown previously to inhibit the ribonucleolytic activity of ANG (Fett et al., 1994), suggesting that it contacts the enzymatic active site. The crystal structure of the Fab complex reveals that the antibody indeed interacts with a key catalytic residue, Lys40, on segment I. Although the contacts formed involve only the alkyl chain of this residue, rather than the Nζ atom that participates in catalysis (Leonidas et al., 1999), binding of the antibody at this position should be sufficient to block access to the active site by RNA substrates.

Experiments to map the binding epitope on ANG in greater detail were performed with an extensive panel of ANG variants and several nonhuman angiogenins (Fett et al., 1994). The results of this study are in complete agreement with the crystal structure. A 300-fold increase in apparent K_d for the complex was observed with an ANG variant (ARH-II) in which residues 38–41 (Pro-Cys-Lys-Asp) are replaced by the corresponding residues of RNase A (Asp-Arg-Cys-Lys-Pro), suggesting that the 38–41 segment of ANG contains an important

Table 3. Potential Hydrogen Bonds between Fab 26-2F and ANG in the Complex Structure

Fab CDR	Fab Residue	ANG Residue	Distance (Å)	Angle (°)
L1	Asn30a Nδ2 (33.8)	Ser37 O (31.9)	2.7	135
	Tyr30b OH (32.2)	Ser37 N (28.2)	3.0	115
		Pro38 O (26.1)	2.6	154
L3	Ser91 O (29.9)	Trp89 Nε1 (28.4)	3.0	174
	Lys92 Nζ (31.1)	Ser37 Oγ (35.3)	2.5	126
		Ser37 O (31.9)	3.2	122
H1	Thr33 Oγ1 (37.1)	Gly86 O (31.9)	3.3	131
H2	Ser52a Oγ (42.1)	Gly85 O (34.0)	3.1	95
	Gly53 N (45.9)	Gly85 O (34.0)	2.9	132
	Asn56 Oδ1 (47.6)	Pro91 O (30.8)	3.3	141
	Tyr58 OH (32.5)	Trp89 O (26.1)	2.9	129
		Trp89 N (27.4)	3.4	162
H3	Tyr100b OH (23.5)	Cys39 O (27.2)	2.8	152

Hydrogen bond parameters were calculated with the program CONTACT (CCP4, 1994). The donor-acceptor cutoff distance is 3.4 Å, and donor-hydrogen-acceptor angles are >90°. The B factors ($Å^2$) of the atoms are given in parentheses.

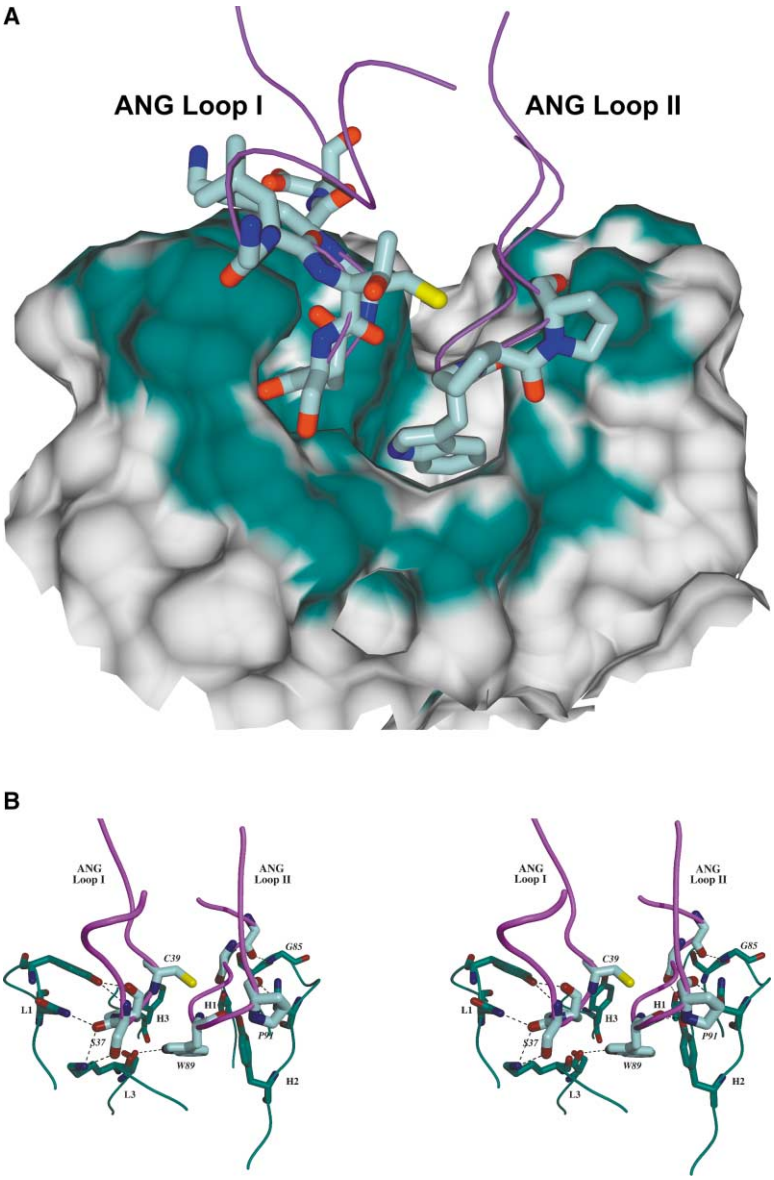

Figure 4. Structural Details of the Interactions at the ANG/Fab 26-2F Interface

(A) The interface region of the complex of Fab 26-2F and ANG, showing the van der Waals surface for the Fab, stick representations (in standard colors) for ANG residues that contact the antibody, and a trace for the ANG backbone (magenta). The CDRs of the Fab, green. The figure was generated with the program DINO (A. Philippsen; http://cobra.mih.unibas.ch/dino/).

(B) Stereo view of the details of the hydrogen bonding contacts in the complex. Hydrogen bonding residues on ANG and the Fab are shown as stick representations, along with their respective backbone traces (magenta and green, respectively). CDRs are labeled in bold type. Potential hydrogen bonds are drawn as broken lines.

part of the binding epitope. These amino acids lie on segment I of the epitope identified in the crystal structure. The substitution should alter its three-dimensional structure (including the main chain) considerably and would therefore eliminate most of the interactions formed by this segment with the antibody. The major role for Trp89 inferred from the crystal structure is supported by the absence of any detectable binding for mouse ANG, in which this Trp is replaced by Arg and all other residues on segments I and II are conserved. An ~3-fold loss in affinity was measured when Trp89 was substituted by a methionine, which can partially fulfill the same function as the Trp in the complex. A minor decrease in affinity was seen for the K40Q variant, consistent with the relatively small role for Lys40 suggested by the crystal structure. Substitutions that involve 26 additional ANG residues outside the structurally defined binding epitope had no significant impact on antibody binding.

Structural Changes in the Cell Binding Region of ANG Due to Fab 26-2F Binding

Remarkably, a segment of ANG (59–68) at the opposite end of the molecule from the Fab combining site adopts a dramatically different conformation in the Fab complex as compared to the free protein (Figure 5) and occupies almost entirely nonoverlapping spaces in the superposed structures (the rmsd for C^{α} atoms is 13.2 Å). In free ANG, residues 62–68 are part of a β hairpin formed by β strands 2 and 3 (residues 62–65 and 69–72, respectively) and the intervening 66–68 loop; residues 59–61 lie on a loop that connects the hairpin structure with α helix 3. In the complex, the β2 strand is lost, and the entire 58–67 segment forms a loop that extends much farther out from the rest of the ANG molecule than does the β hairpin. The structure of this loop appears to be maintained by nine intraloop hydrogen bonds and two hydrogen bonds with outside residues (Arg5 and Arg70).

The 60–68 segment of ANG has been demonstrated

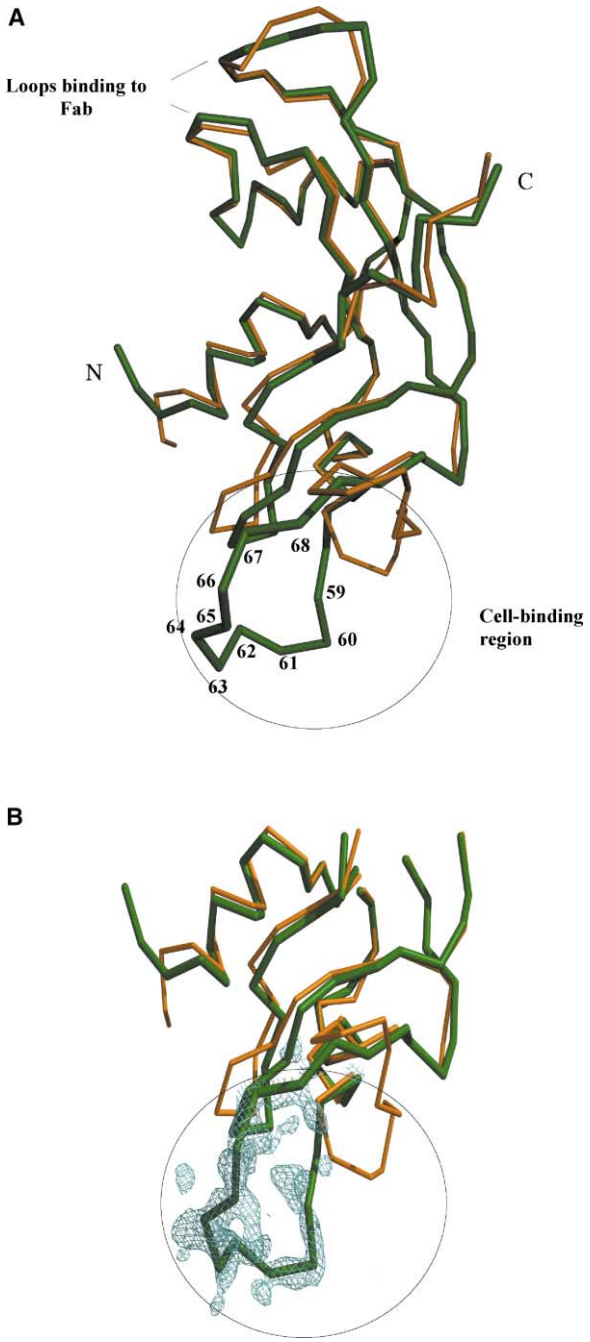

Figure 5. Superposition of the C^{α} Atoms of Free ANG (Protein Data Bank Code 1B1I; Orange) and ANG from the Fab 26-2F Complex (Dark Green)

The two loops that contact the Fab are indicated. The region containing cell binding site residues 60–68 is circled and shown below with a portion of the $F_o - F_c$ electron density map clearly showing the deviation in the conformation of this region in Fab-bound ANG. The map is contoured at 3.0 σ. The figure was created with BOBSCRIPT (Esnouf, 1997) and RASTER 3D (Merritt and Bacon, 1997).

previously to play a critical functional role that is independent of catalysis. Cleavage of the 60/61 or 67/68 peptide bond (Hallahan et al., 1991), deamidation of Asn61 (Hallahan et al., 1992), and Ala substitution of Arg66 (Shapiro and Vallee, 1992) all abolish angiogenic activity without influencing ribonucleolytic activity appreciably, and most of the angiogenically inactive derivatives have been shown to lack the capacity to inhibit ANG-induced angiogenesis (in contrast with angiogenically inactive catalytic site variants). On the basis of these findings, the region containing the 60–68 segment was proposed to constitute a cell binding site. The endothelial cell targets of ANG display at least two molecules on their surface (an ANG receptor and an ANG binding protein [ANGBP] in the actin family) that participate in the angiogenic mechanism (Hu and Riordan, 1993; Hu et al., 1993, 1997), and modifications within the 60–68 segment impede the interactions with both of them (Hu et al., 1991; G.-f.H. and R.S., unpublished data). This region most likely does not retain any significant affinity for cellular targets when it adopts the conformation seen in the Fab complex. It is therefore of considerable interest to ascertain whether this restructuring is triggered by the binding of the antibody or whether it is a consequence of packing in the crystal.

To the best of our knowledge, there is no precedent for crystallization causing such a drastic structural reorganization, involving the destruction of a well-ordered region of the secondary structure (as opposed to the reshaping of a flexible loop). Clearly, the conformation of the 59–68 segment in the free ANG crystal structure is not determined by crystal packing; the NMR solution structure (all 30 sets of coordinates; Lequin et al., 1997) shows a high degree of similarity in this region, as do the crystal structures of wild-type bovine ANG and all seven human ANG variants examined to date (Acharya et al., 1994, 1995; Leonidas et al., 1999, 2002). Moreover, it seems unlikely that the conformation of this segment in the Fab complex is dictated by crystal contacts; although ANG residues 62, 64, and 65 pack against C_L of the Fab in a symmetry-related molecule, only a single hydrogen bond is formed, and the other interactions (all van der Waals, with little burying of hydrophobic groups) are not expected to provide much energy for stabilization. However, inspection of the free ANG and ANG-Fab structures does not reveal any obvious mechanism by which attachment of the Fab to segments I and II would induce the restructuring of the cell binding region more than 20 Å away.

Direct evidence that binding of mAb 26-2F induces the observed conformational change was obtained by examining the effect of the antibody on the interaction of ANG with ANGBP in solution (Figure 6). ^{125}I-ANG can be readily crosslinked to endothelial cell ANGBP, producing a band with an apparent M_r of 58,000 during SDS-PAGE (Hu et al., 1991) (lane 2). The intensity of this band is reduced by 65% $\pm$ 5% (results of three independent experiments) if the labeled ANG is preincubated with a 10-fold molar excess of mAb 26-2F prior to addition of the binding protein and crosslinking reagent (lane 4). This effect does not reflect crosslinking of ANG to the mAb because only a small amount of crosslinked ANG-mAb complex is observed when the ANG binding protein is omitted (lane 3), and there is no band at the expected position of the ternary complex when all three components are included (lane 4). Moreover, preincubation with two other mAbs (36u and 32-B5) has no effect

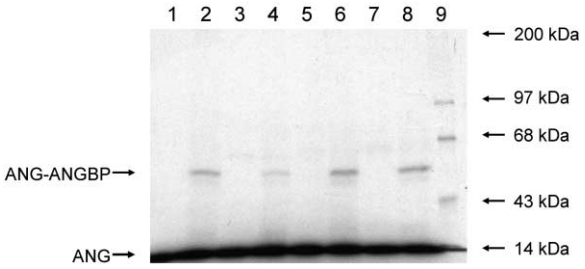

Figure 6. Effect of mAb 26-2F on the Binding of ANG to ANG Binding Protein (ANGBP)

^{125}I-ANG was incubated for 30 min in the presence or absence of a 10-fold molar excess of mAb prior to addition of ANGBP or PBS. After 10 min of further incubation, samples were subjected to crosslinking with carbodiimide and then analyzed by SDS-PAGE and autoradiography. Lane 1, ANG alone; lane 2, ANG plus ANGBP; lanes 3, 5, and 7, ANG plus mAb 26-2F, 36u, or 32-B5, respectively; lanes 4, 6, and 8, ANG plus mAb (26-2F, 36u, and 32-B5, respectively) and ANGBP; lane 9, molecular weight standards. The extent of the reduction in crosslinking of ANG to ANGBP due to preincubation with mAB 26-2F (lane 4 versus lane 2) in this experiment, as determined by densitometry, is 70%.

on the intensity of the 58 kDa band (lanes 6 and 8), even when used in 300-fold molar excess (data not shown). The affinities of 36u and 32-B5 for the ANG variants ARH-II, W89M, and K40Q are indistinguishable from those of ANG (K.A.O. and J.W.F., unpublished data), demonstrating that the epitopes of these mAbs are distinct from that of 26-2F. The effect of mAb 26-2F on crosslinking of ANG to ANGBP strongly suggests that binding of the antibody alters the conformation of the ANGBP binding site. However, it remains to be determined whether or not this structural change corresponds to that seen in the crystal structure of the ANG-Fab 26-2F complex.

Biological Implications

Monoclonal antibody 26-2F has been used successfully in preclinical mouse models to inhibit the establishment and/or metastatic dissemination of human colon, lung, fibroblast, breast, and prostate tumors (Olson et al., 1994, 1995, 2002; Piccoli et al., 1998). The determination of the 3D structure of the ANG-Fab complex now provides the information required to rationally construct a maximally humanized version of 26-2F for potential clinical use against cancer. Specifically, the structure suggests that it may be sufficient to graft only four of the six CDRs (L1, L3, H2, and H3) from the mouse antibody onto the human framework, since CDR-L2 forms no contacts and CDR-H1 makes only one interaction. The structure also identifies five framework residues from the mouse protein that may be required to enhance the avidity of a humanized IgG1κ Fab; H47 (Trp) and H71 (Arg) interact with CDR-H2 residues that participate in the interface, and L49 (Tyr), H94 (Arg), and H103 (Trp) all appear to help stabilize the conformation of CDR-H3. A humanized Fab of the type just described would contain less than 13% murine-derived sequence and would therefore be minimally immunogenic in patients. The 3D structure of the ANG-Fab complex may also aid in the design of peptide mimetic, small-molecule inhibitors based on the critical CDR residues that contact ANG. This approach has been used previously for other antibodies (see Berezov et al., 2001, and references therein).

A completely unexpected feature of the ANG-Fab 26-2F structure was the marked perturbation of the cell binding site of ANG induced by attachment of the antibody. Earlier work on mAb 26-2F had correctly identified the region of ANG containing residues 38–41 and 89 (i.e., the region most distant from the cell binding site) as the binding epitope, and had indicated that neutralization of the angiogenic activity was due to inhibition of the ribonucleolytic activity of ANG. It now appears that the antibody disables ANG via a second, indirect route as well, i.e., by destroying the native conformation of a segment that is critical for the interactions of ANG with surface components on its endothelial cell targets.

Experimental Procedures

ANG Production and Preparation of mAb 26-2F and Its Fab Fragment

<Glu-1 human ANG was produced with a recombinant system in *Escherichia coli* (Shapiro et al., 1988) and dissolved in water to a concentration of 20 mg/ml. mAb 26-2F was obtained from ascites fluid as described previously (Fett et al., 1994) and was dialyzed extensively against 20 mM sodium phosphate (pH 7.0) and 10 mM EDTA. Fab fragments were prepared by papain digestion with an ImmunoPure Fab Preparation Kit (Pierce, Rockford, IL). Purity was confirmed by SDS-PAGE, and the final products were dialyzed against a 1:150 dilution of phosphate-buffered saline (pH 7.2) and concentrated to 20 mg/ml with a Centricon Plus-20 ultrafiltration device (Millipore, Bedford, MA).

Crystallization and Data Collection for the Fab-ANG Complex

The Fab-ANG complex was formed by mixing Fab and ANG in a 1:1.2 molar ratio and incubating overnight at 4°C. Crystals were grown at 16°C by the hanging drop vapor diffusion technique with 30% PEG 8000 and 0.2 M Li_2SO_4 (pH 6.0–7.5) as the reservoir solution. A full data set to 2.0 Å resolution was collected on station PX 9.6 of the SRS, Daresbury (UK), at 100 K from one crystal (with 20% [v/v] glycerol in the reservoir buffer). This data set, merged with a 3.5 Å low-resolution data set collected with the same crystal, had an R_{sym} value of 6.1% and 98.9% overall completeness. The details of data processing statistics are shown in Table 1. The programs DENZO and SCALEPACK were used for data integration and scaling (Otwinowski and Minor, 1997).

Structure Determination

The structure was solved by molecular replacement with AmoRe (Navaza, 1994). Different models for the V and the C regions from the Protein Data Bank were used in the search. Consistent peaks were found for most of the V domain models at (x, y, z) = (0.33, 0.00, 0.19). The best model selected from the rotation function was humanized anti-p185HER2 antibody 4D5 (Protein Data Bank code 1FVC; Eigenbrot et al., 1993) (correlation coefficient of 18.3 for the first peak and 9.9 for the second). Models for the C domain gave a consistent peak in the translation function at (0.06, 0.00, 0.25), and the best models in the rotation functions were the C domains of the Fab fragments of mAbs HyHel-5 (Protein Data Bank code 3HFL; Cohen et al., 1996) (first peak 1.44 σ higher than the second peak) and TE33 (Protein Data Bank code 1TET; Shoham, 1993) (first peak 1.63 σ higher than the second peak). At this stage, the 1TET C domain was fixed, and the rotation peaks from the 1FVC model were used in order to find the position of the V domain. This search resulted in a correlation coefficient of 45.1% and an R factor of 48.0%. No symmetry-related clashes were observed, and the V and C domains were found as expected for an antibody molecule. In the next step, the V and C domains were fixed, and a translation search was performed to locate the position of the ANG molecule. The correlation coefficient at this stage went up to 51.8% and the

R factor dropped further to 45.8% for the three components. Examination of the ANG position with the program O (Jones et al., 1991) showed that it was indeed located in a suitable position to contact the CDRs of the Fab.

Structure Refinement

Structure refinement was carried out with the molecular replacement model with CNS 1.0 (Brünger et al., 1998) by gradual extension to 2.0 Å, with molecular dynamics at 2000 K followed by Powell energy minimization. Map calculations were performed with CNS with all reflections in the resolution range 40.0–2.0 Å. Significant changes in the structure were observed during the refinement. Most notably, there was a large movement of the ANG region containing residues 60–69, with the altered conformation extending into the solvent. Additionally, it was necessary to model residues 195–199 in C_L, 71–76 and 100–102 in V_H, and 187–191 in C_H in a different conformation, and an extended loop region in C_H from 128 to 133 had to be modeled de novo. Finally, five residues of the hinge region that joins the Fab and Fc portions of the antibody were modeled with the aid of the $F_o - F_c$ electron density map (Harris et al., 1998). Water molecules were incorporated into the structure if they had peak heights $>3\ \sigma$ in the $F_o - F_c$ difference electron density maps and were within hydrogen bonding distance of appropriate atoms. Six molecules of glycerol from the cryoprotectant and eight sulfate ions were also identified in the structure and were included in the final stages of refinement. Model refinement statistics and stereochemical parameters are given in Table 1.

Effect of mAbs on Crosslinking of ANG to ANG Binding Protein

Crosslinking was carried out essentially as described previously (Hu et al., 1991). ^{125}I-ANG, 0.1 μg, was incubated for 10 min at room temperature in the presence or absence of 10 μg of mAb (26-2F, 36u, or 32-B5) in 40 μl of PBS. An endothelial cell surface extract containing ANGBP (Hu et al., 1991) or PBS, 10 μl, was then added, and the mixtures were incubated for another 10 min, and then 1-ethyl-3-(3-dimethylaminopropyl) carbodiimide crosslinker was added to a final concentration of 10 mM. After 30 min at room temperature, the reaction was quenched by the addition of Tris-HCl to 100 mM. Samples were then subjected to SDS-PAGE separation (10% acrylamide), and radiolabeled bands were visualized by autoradiography. Band intensities were quantified by densitometry (Hu et al., 1991).

Acknowledgments

This work was supported by Cancer Research UK (project grant SP2354/0102), the Wellcome Trust (UK) (programme grant 067288 to K.R.A.), and the National Institutes of Health (grant CA60046 to J.W.F.). We are grateful to the staff at the Synchrotron Radiation Sources at Daresbury (UK) and the ESRF, Grenoble (France), BM14 for their help during X-ray data collection.

Received: December 12, 2002
Revised: February 25, 2003
Accepted: March 27, 2003
Published: July 1, 2003

References

Acharya, K.R., Shapiro, R., Allen, S.C., Riordan, J.F., and Vallee, B.L. (1994). Crystal structure of human angiogenin reveals the structural basis for its functional divergence from ribonuclease. Proc. Natl. Acad. Sci. USA *91*, 2915–2919.

Acharya, K.R., Shapiro, R., Riordan, J.F., and Vallee, B.L. (1995). Crystal structure of bovine angiogenin at 1.5 Å resolution. Proc. Natl. Acad. Sci. USA *92*, 2949–2953.

Adams, S.A., and Subramanian, V. (1999). The angiogenins: an emerging family of ribonuclease related proteins with diverse cellular functions. Angiogenesis *3*, 189–199.

Al-Lazikani, B., Lesk, A.M., and Chothia, C. (1997). Standard conformations for the canonical structures of immunoglobulins. J. Mol. Biol. *273*, 927–948.

Berezov, A., Zhang, H.T., Greene, M.I., and Murali, R. (2001). Disabling erbB receptors with rationally designed exocyclic mimetics of antibodies: structure-function analysis. J. Med. Chem. *44*, 2565–2574.

Braden, B.C., Souchon, H., Eisele, J.L., Bentley, G.A., Bhat, T.N., Navaza, J., and Poljak, R.J. (1994). Three-dimensional structures of the free and the antigen-complexed Fab from monoclonal antilysozyme antibody D44.1. J. Mol. Biol. *243*, 767–781.

Brünger, A.T., Adams, P.D., Clore, G.M., DeLano, W.L., Gros, P., Grosse-Kunstleve, R.W., Jiang, J.S., Kuszewski, J., Nilges, M., Pannu, N.S., et al. (1998). Crystallography and NMR system: a new software suite for macromolecular structure determination. Acta Crystallogr. D Biol. Crystallogr. *54*, 905–921.

Carter, P. (2001). Improving the efficacy of antibody-based cancer therapies. Nat. Rev. Cancer *1*, 118–129.

CCP4 (Collaborative Computational Project 4). (1994). The CCP4 suite: programs for protein crystallography. Acta Crystallogr. D Biol. Crystallogr. *50*, 760–763.

Chothia, C., and Lesk, A.M. (1987). Canonical structures for the hypervariable regions of immunoglobulins. J. Mol. Biol. *196*, 901–917.

Chothia, C., Lesk, A.M., Tramontano, A., Levitt, M., Smith-Gill, S.J., Air, G., Sheriff, S., Padlan, E.A., Davies, D., Tulip, W.R., et al. (1989). Conformations of immunoglobulin hypervariable regions. Nature *342*, 877–883.

Choy, E.H., Kingsley, G.H., and Panayi, G.S. (1993). Treatment with anti-CD4 monoclonal antibody and acute interstitial nephritis. Arthritis Rheum. *36*, 723–724.

Choy, E.H.S., Schantz, A., Woody, J., Kingsley, G.H., and Panayi, G.S. (1994). Human anti-chimeric antibody response in rheumatoid arthritis patients treated with a chimeric anti-CD4 monoclonal antibody. Arthritis Rheum. *37*, S340.

Cohen, G.H., Sheriff, S., and Davies, D.R. (1996). Refined structure of the monoclonal antibody HyHel-5 with its antigen hen egg white lysozyme. Acta Crystallogr. D Biol. Crystallogr. *52*, 315–326.

Davies, D.R., and Cohen, G.H. (1996). Interactions of protein antigens with antibodies. Proc. Natl. Acad. Sci. USA *93*, 7–12.

Eberle, K., Oberpichler, A., Trantakis, C., Krupp, W., Knupfer, M., Tschesche, H., and Seifert, V. (2000). The expression of angiogenin in tissue samples of different brain tumors and cultured glioma cells. Anticancer Res. *20*, 1679–1684.

Eigenbrot, C., Randal, M., Presta, L., Carter, P., and Kossiakoff, A.A. (1993). X-ray structures of the antigen-binding domains from three variants of humanized anti-p185HER2 antibody 4D5 and comparison with molecular modeling. J. Mol. Biol. *229*, 969–995.

Esnouf, R.M. (1997). An extensively modified version of Molscript that includes greatly enhanced coloring capabilities. J. Mol. Graph. *15*, 132–134.

Fett, J.W., Strydom, D.J., Lobb, R.R., Alderman, E.M., Bethune, J.L., Riordan, J.F., and Vallee, B.L. (1985). Isolation and characterization of angiogenin, an angiogenic protein from human carcinoma cells. Biochemistry *24*, 5480–5486.

Fett, J.W., Olson, K.A., and Rybak, S.M. (1994). A monoclonal antibody to human angiogenin. Inhibition of ribonucleolytic and angiogenic activities and localization of the antigenic epitope. Biochemistry *33*, 5421–5427.

Foote, J., and Winter, G. (1992). Antibody framework residues affecting the conformation of the hypervariable loops. J. Mol. Biol. *224*, 487–499.

Hallahan, T.W., Shapiro, R., and Vallee, B.L. (1991). Dual site model for the organogenic activity of angiogenin. Proc. Natl. Acad. Sci. USA *88*, 2222–2226.

Hallahan, T.W., Shapiro, R., Strydom, D.J., and Vallee, B.L. (1992). Importance of asparagine-61 and asparagine-109 to the angiogenic activity of human angiogenin. Biochemistry *31*, 8022–8029.

Harris, L.J., Skaletsky, E., and McPherson, A. (1998). Crystallo-

graphic structure of an intact IgG1 monoclonal antibody. J. Mol. Biol. *275*, 861–872.

Hu, G.-f., and Riordan, J.F. (1993). Angiogenin enhances actin acceleration of plasminogen activation. Biochem. Biophys. Res. Commun. *197*, 682–687.

Hu, G.-f., Chang, S.I., Riordan, J.F., and Vallee, B.L. (1991). An angiogenin-binding protein from endothelial cells. Proc. Natl. Acad. Sci. USA *88*, 2227–2231.

Hu, G.-f., Strydom, D.J., Fett, J.W., Riordan, J.F., and Vallee, B.L. (1993). Actin is a binding protein for angiogenin. Proc. Natl. Acad. Sci. USA *90*, 1217–1221.

Hu, G.-f., Riordan, J.F., and Vallee, B.L. (1997). A putative angiogenin receptor in angiogenin-responsive human endothelial cells. Proc. Natl. Acad. Sci. USA *94*, 2204–2209.

Jones, S., and Thornton, J.M. (1996). Principles of protein-protein interactions. Proc. Natl. Acad. Sci. USA *93*, 13–20.

Jones, T.A., Zou, J.Y., Cowan, S.W., and Kjeldgaard, M. (1991). Improved methods for building models in electron density maps and the location of errors in these models. Acta Crystallogr. A *47*, 110–119.

Kabat, E.A., Wu, T.T., Perry, H.M., Gottesman, K.S., and Foeller, C. (1991). Sequences of Proteins of Immunological Interest, Fifth Edition (Bethesda, MD: U.S. Department of Health and Human Services).

Kraulis, P.J. (1991). MOLSCRIPT—a program to produce both detailed and schematic plots of protein structures. J. Appl. Crystallogr. *24*, 946–950.

Laskowski, R.A., MacArthur, M.W., Moss, D.S., and Thornton, J.M. (1993). PROCHECK—a program to check the stereochemical quality of protein structures. J. Appl. Crystallogr. *26*, 283–291.

Leonidas, D.D., Shapiro, R., Allen, S.C., Subbarao, G.V., Veluraja, K., and Acharya, K.R. (1999). Refined crystal structures of native human angiogenin and two active site mutants: implications for the unique functional properties of an enzyme involved in neovascularization during tumor growth. J. Mol. Biol. *285*, 1209–1233.

Leonidas, D.D., Shapiro, R., Subbarao, G.V., Russo, A., and Acharya, K.R. (2002). Crystallographic studies on the role of the C-terminal segment of human angiogenin in defining enzymatic potency. Biochemistry *41*, 2552–2562.

Lequin, O., Albaret, C., Bontems, F., Spik, G., and Lallemand, J.Y. (1996). Solution structure of bovine angiogenin by ^{1}H nuclear magnetic resonance spectroscopy. Biochemistry *35*, 8870–8880.

Lequin, O., Thuring, H., Robin, M., and Lallemand, J.-Y. (1997). Three-dimensional solution structure of human angiogenin determined by ^{1}H, ^{15}N-NMR spectroscopy. Characterisation of histidine protonation states and pK_a values. Eur. J. Biochem. *250*, 712–726.

Levy, R., and Miller, R.A. (1983). Biological and clinical implications of lymphocyte hybridomas: tumor therapy with monoclonal antibodies. Annu. Rev. Med. *34*, 107–116.

Li, D., Bell, J., Brown, A., and Berry, C.L. (1994). The observation of angiogenin and basic fibroblast growth factor gene expression in human colonic adenocarcinomas, gastric adenocarcinomas, and hepatocellular carcinomas. J. Pathol. *172*, 171–175.

Lobuglio, A.F., Saleh, M., Peterson, L., Wheeler, R., Carrano, R., Huster, W., and Khazaeli, M.B. (1986). Phase I clinical trial of CO17-1A monoclonal antibody. Hybridoma *1*, S117–S123.

Maes, P., Damart, D., Rommens, C., Montreuil, J., Spik, G., and Tartar, A. (1988). The complete amino acid sequence of bovine milk angiogenin. FEBS Lett. *241*, 41–45.

Mas, M.T., Smith, K.C., Yarmush, D.L., Aisaka, K., and Fine, R.M. (1992). Modeling the anti-CEA antibody combining site by homology and conformational search. Proteins *14*, 483–498.

Merritt, E.A., and Bacon, D.J. (1997). Raster3D photorealistic molecular graphics. Methods Enzymol. *277*, 505–524.

Morea, V., Tramontano, A., Rustici, M., Chothia, C., and Lesk, A.M. (1998). Conformations of the third hypervariable region in the VH domain of immunoglobulins. J. Mol. Biol. *275*, 269–294.

Navaza, J. (1994). AMoRe: an automated package for molecular replacement. Acta Crystallogr. A *50*, 157–163.

Olson, K.A., French, T.C., Vallee, B.L., and Fett, J.W. (1994). A monoclonal antibody to human angiogenin suppresses tumor growth in athymic mice. Cancer Res. *54*, 4576–4579.

Olson, K.A., Fett, J.W., French, T.C., Key, M.E., and Vallee, B.L. (1995). Angiogenin antagonists prevent tumor growth in vivo. Proc. Natl. Acad. Sci. USA *92*, 442–446.

Olson, K.A., Byers, H.R., Key, M.E., and Fett, J.W. (2002). Inhibition of prostate carcinoma establishment and metastatic growth in mice by an antiangiogenin monoclonal antibody. Int. J. Cancer *98*, 923–929.

Otwinowski, Z., and Minor, W. (1997). Processing of X-ray diffraction data collected in oscillation mode. Methods Enzymol. *276*, 307–326.

Padlan, E.A. (1990). On the nature of antibody combining sites: unusual structural features that may confer on these sites an enhanced capacity for binding ligands. Proteins *7*, 112–124.

Piccoli, R., Olson, K.A., Vallee, B.L., and Fett, J.W. (1998). Chimeric anti-angiogenin antibody cAb 26–2F inhibits the formation of human breast cancer xenografts in athymic mice. Proc. Natl. Acad. Sci. USA *95*, 4579–4583.

Presta, L.G., Chen, H., O'Connor, S.J., Chisholm, V., Meng, Y.G., Krummen, L., Winkler, M., and Ferrara, N. (1997). Humanization of an anti-vascular endothelial growth factor monoclonal antibody for the therapy of solid tumors and other disorders. Cancer Res. *57*, 4593–4599.

Queen, C., Schneider, W.P., Selick, H.E., Payne, P.W., Landolfi, N.F., Duncan, J.F., Avdalovic, N.M., Levitt, M., Junghans, R.P., and Waldmann, T.A. (1989). A humanized antibody that binds to the interleukin 2 receptor. Proc. Natl. Acad. Sci. USA *86*, 10029–10033.

Riechmann, L., Clark, M., Waldmann, H., and Winter, G. (1988). Reshaping human antibodies for therapy. Nature *332*, 323–327.

Riordan, J.F. (1997). Structure and function of angiogenin. In Ribonucleases: Structure and Functions, G. D'Alessio and J.F. Riordan, eds. (New York: Academic Press), pp. 445–489.

Rybak, S.M., Fett, J.W., Yao, Q.Z., and Vallee, B.L. (1987). Angiogenin mRNA in human tumor and normal cells. Biochem. Biophys. Res. Commun. *146*, 1240–1248.

Schneider, W.P., Wensel, T.G., Stryer, L., and Oi, V.T. (1988). Genetically engineered immunoglobulins reveal structural features controlling segmental flexibility. Proc. Natl. Acad. Sci. USA *85*, 2509–2513.

Shapiro, R., and Vallee, B.L. (1989). Site-directed mutagenesis of histidine-13 and histidine-114 of human angiogenin. Alanine derivatives inhibit angiogenin-induced angiogenesis. Biochemistry *28*, 7401–7408.

Shapiro, R., and Vallee, B.L. (1992). Identification of functional arginines in human angiogenin by site-directed mutagenesis. Biochemistry *31*, 12477–12485.

Shapiro, R., Riordan, J.F., and Vallee, B.L. (1986). Characteristic ribonucleolytic activity of human angiogenin. Biochemistry *25*, 3527–3532.

Shapiro, R., Strydom, D.J., Olson, K.A., and Vallee, B.L. (1987). Isolation of angiogenin from normal human plasma. Biochemistry *26*, 5141–5146.

Shapiro, R., Harper, J.W., Fox, E.A., Jansen, H.W., Hein, F., and Uhlmann, E. (1988). Expression of Met-(−1) angiogenin in *Escherichia coli*: conversion to the authentic <Glu-1 protein. Anal. Biochem. *175*, 450–461.

Shapiro, R., Fox, E.A., and Riordan, J.F. (1989). Role of lysines in human angiogenin: chemical modification and site-directed mutagenesis. Biochemistry *28*, 1726–1732.

Sheriff, S., Jeffrey, P.D., and Bajorath, J. (1996). Comparison of CH1 domains in different classes of murine antibodies. J. Mol. Biol. *263*, 385–389.

Shimoyama, S., Gansauge, F., Gansauge, S., Negri, G., Oohara, T., and Beger, H.G. (1996). Increased angiogenin expression in pancreatic cancer is related to cancer aggressiveness. Cancer Res. *56*, 2703–2706.

Shirai, H., Kidera, A., and Nakamura, H. (1996). Structural classification of CDR-H3 in antibodies. FEBS Lett. *399*, 1–8.

Shoham, M. (1993). Crystal structure of an anticholera toxin peptide complex at 2.3 Å. J. Mol. Biol. *232*, 1169–1175.

Sogabe, S., Stuart, F., Henke, C., Bridges, A., Williams, G., Birch, A., Winkler, F.K., and Robinson, J.A. (1997). Neutralizing epitopes on the extracellular interferon γ receptor (IFNγR) α-chain characterized by homolog scanning mutagenesis and X-ray crystal structure of the A6 Fab-IFNγR1–108 complex. J. Mol. Biol. *273*, 882–897.

Strydom, D.J., Fett, J.W., Lobb, R.R., Alderman, E.M., Bethune, J.L., Riordan, J.F., and Vallee, B.L. (1985). Amino acid sequence of human tumor derived angiogenin. Biochemistry *24*, 5486–5494.

Whitelegg, N.R., and Rees, A.R. (2000). WAM: an improved algorithm for modelling antibodies on the WEB. Protein Eng. *13*, 819–824.

Wilson, I.A., and Stanfield, R.L. (1994). Antibody-antigen interactions: new structures and new conformational changes. Curr. Opin. Struct. Biol. *4*, 857–867.

Accession Numbers

The atomic coordinates for the ANG-Fab complex have been deposited with the Protein Data Bank under accession code 1H0D.